Electrical and structural properties of $In_xGa_{1-x}N$ on GaAs

C. R. Abernathy, J. D. MacKenzie, S. R. Bharatan, K. S. Jones, and S. J. Pearton
Department of Materials Science and Engineering, University of Florida, Gainesville, Florida 32611

(Received 7 November 1994; accepted for publication 31 January 1995)

$In_xGa_{1-x}N$ ($x=0.07-1.0$) layers were grown on GaAs substrates by metalorganic molecular beam epitaxy. The films display strong *n*-type conductivity ($n>10^{20}$ cm^{-3}) for a wide range of compositions. The use of an H_2 rather than a He carrier gas produces a lower carrier concentration in the as-grown material. The $In_xGa_{1-x}N$ is single crystal at low Ga concentrations with the lattice mismatch accommodated by a high density of stacking faults and microtwins. The InN layers contain only the cubic phase, while the ternaries contain both cubic and hexagonal phases.

The recent development of InGaN/GaN blue light-emitting diodes has intensified interest in the growth and properties of the wide band-gap nitrides.[1] Several groups have reported stimulated emission from optically pumped InGaN/GaN heterostructures[2,3] and a critical evaluation of the potential for wide band-gap compounds for high power electronic devices indicates that InGaN and related ternaries are well suited for high-temperature operation.[4] Most of the $In_xGa_{1-x}N$ reported to date has been grown by organometallic vapor phase epitaxy (OMVPE) with device quality material generally being grown at ~800 °C.[1–3,5–7] There is interest in $In_xGa_{1-x}N$ grown by other techniques, including metalorganic molecular beam epitaxy, with the potential for more selective deposition or higher doping levels as found in other III–V materials. In this letter we report the growth of $In_xGa_{1-x}N$ grown by metalorganic molecular beam epitaxy (MOMBE) on (100) GaAs paying particular attention to the variation of the structural and electrical properties with composition.

The samples were grown on semi-insulating, (100) GaAs substrates at 500 °C in an Intevac Gas Source Gen II. Triethylgallium (TEG) and trimethylindium (TMI) were transported by either H_2 or He carrier gases in order to examine possible hydrogen passivation effects, a common problem in OMVPE-grown GaN films.[8,9] An electron cyclotron resonance plasma source (Wavemat MPDR 610) operating at 2.45 GHz and 200 W forward power was used to provide the nitrogen flux. Optical emission spectroscopy indicates that a significant atomic nitrogen fraction is produced under these conditions though the presence of peaks at 335, 326, 390, and 391 nm shows there to be some N_2 and N_2^+, respectively, in the beam. The film compositions were varied by altering the relative group III gas flow rates. Further details of the growth system have been given previously.[10]

The electrical transport properties of the $In_xGa_{1-x}N$ films were obtained from Van der Pauw geometry Hall measurements at 300 K using alloyed (400 °C, 2 min) HgIn ohmic contacts. The composition of the samples was determined by electron microprobe analysis using a 6 kV beam. Surface morphology was examined by scanning electron microscopy (SEM) and cross-section transmission electron microscopy (TEM) was used for the defect analysis. Both x-ray diffraction (XRD) and selected area diffraction patterns (SADPs) were used to distinguish the wurtzite and zincblende phases.

Figure 1 shows the carrier concentration and mobility at room temperature in the $In_xGa_{1-x}N$ as a function of the experimentally determined In mole fraction. The pure InN grown with either H_2 or He carrier gas is strongly *n*-type ($\sim 3\times10^{20}$ cm^{-3}). High *n*-type doping levels have also been observed in InN prepared by other methods. The source of this autodoping is usually ascribed to the presence of In vacancies,[11,12] though this seems less likely in light of the trends observed in InN grown using various V/III ratios.[10] The material retains carrier concentrations above $\sim10^{20}$ cm^{-3} over the composition range InN to $\sim In_{0.2}Ga_{0.8}N$, at which point there is a sharp fall-off in the autodoping level. Note however, that the fall-off is more dramatic in material grown with the H_2 carrier gas and this may be due to hydrogen passivation of the defects responsible for the *n*-type conductivity. We have similar effects in InN films directly exposed to H_2 plasmas, where reductions in carrier concentration were measured when atomic hydrogen was incorporated into the material.[13] The electron mobility generally decreases with decreasing In content in the $In_xGa_{1-x}N$, corresponding to increasing band gap.

The SEM micrographs in Fig. 2 show the effect of increasing Ga content on the morphology of $In_xGa_{1-x}N$ grown at 500 °C. For a Ga mole fraction of 0.33 the surface is essentially specular (top) while as the TEG flux is increased at constant TMI flow rate to produce Ga mole fractions of 0.47 (center) or 0.63 (bottom), the morphology degrades. GaN grown under the conditions used for the InGaN gener-

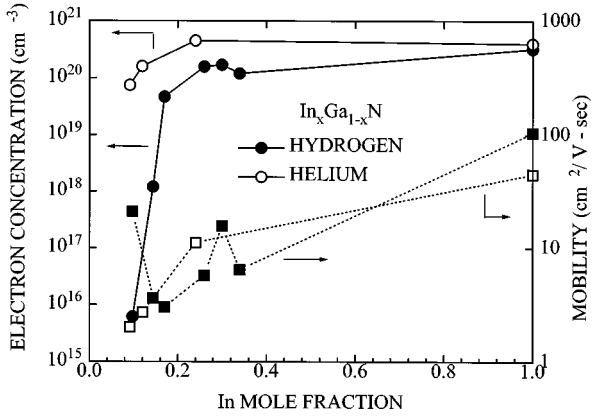

FIG. 1. Electron concentration and mobility at 300 K in $In_xGa_{1-x}N$ films grown at 500 °C on GaAs as a function of ternary composition.

 0003-6951/95/66(13)/1632/3/$6.00 © 1995 American Institute of Physics

Downloaded¬25¬Mar¬2011¬to¬128.227.207.19.¬Redistribution¬subject¬to¬AIP¬license¬or¬copyright;¬see¬http://apl.aip.org/about/rights_and_permissions

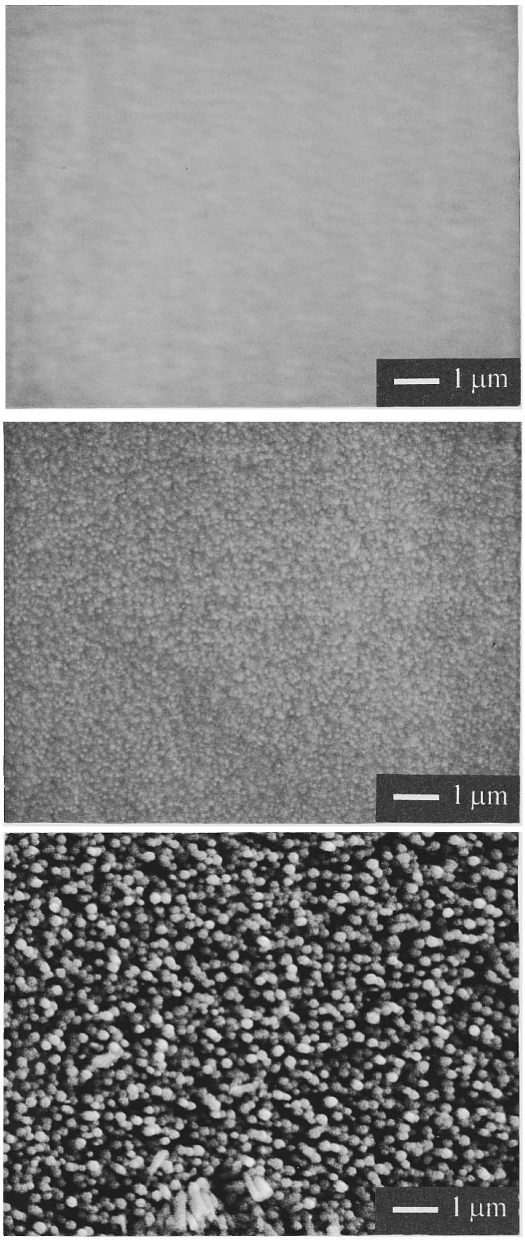

FIG. 2. SEM micrographs of InGaN films. Ga mole fraction increases from (top) 0.33 to (center) ~0.53 to (bottom) ~0.64. Layers were grown on GaAs at 500 °C using the same TMI flow rates.

ally produces polycrystalline layers with morphologies similar to or worse than those shown in Fig. 2. Temperatures of ~700 °C are normally used to suppress this surface roughness. However, though higher temperatures may improve the surfaces of the InGaN layers with higher Ga content, the composition may become difficult to control due to desorption of In at $T>450$ °C. Further work is needed to determine the optimum trade-off of temperature in terms of morphology and reproducibility.

XRD of the films showed that InN grown at a rate of 70 Å/min was cubic or β phase, while the ternaries contained both cubic and hexagonal or α phases. Since only (002)-type peaks from the film and substrate were visible in the $\theta/2\theta$ to powder diffractometer scans, this indicates the crystallographic orientation relationship is (001) GaAs‖(0001) α-$In_xGa_{1-x}N$‖(001) β-$In_xGa_{1-x}N$. Figure 3 (top) shows a bright field cross-sectional TEM micrograph of the InN layer obtained using two beam diffraction conditions with diffraction vector $g=[220]$ of the GaAs substrate. Stacking faults laying along the {111} planes are the main defects present. The SADP of the episubstrate region is shown in the upper right-hand corner of the micrograph, and using standard indexing methods the film–substrate orientation relationship was determined as (001) GaAs‖(001) β-InN and [011] GaAs‖[011] β-InN. The diffuse scattering visible in the SADP is due to the high stacking fault density in the InN. A cross-sectional TEM micrograph of an $In_{0.26}Ga_{0.74}N$ layer on GaAs is shown at the bottom of Fig. 3. The material is again defective single crystal and high-resolution microscopy showed that microtwins and stacking faults were the major structural imperfections. We observed qualitatively that the defect density was higher in the InGaN relative to InN, again suggesting that the growth temperature must be increased with increasing Ga content in order to maintain reasonable crystal quality.

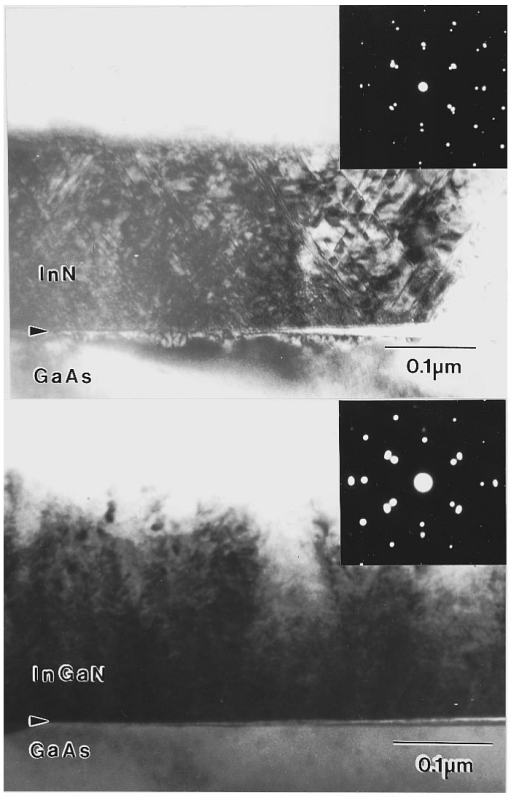

FIG. 3. Cross-section TEM micrographs and selected area diffraction patterns from InN (top) and $In_{0.26}Ga_{0.74}N$ (bottom) samples grown directly on GaAs. The TEM was performed under bright-field, $g=[220]$ conditions.

In conclusion, we find strong n-type conductivity in $In_xGa_{1-x}N$ grown on GaAs by MOMBE, even for low In mole fractions. This autodoping is lower in samples grown with a H_2 carrier gas compared to samples grown with He. The InN layers are single crystal, but contain a high density of stacking faults and microtwins due to the mismatch with the GaAs substrate.

The authors acknowledge the technical support of the

Downloaded¬25¬Mar¬2011¬to¬128.227.207.19.¬Redistribution¬subject¬to¬AIP¬license¬or¬copyright;¬see¬http://apl.aip.org/about/rights_and_permissions

staff of the Microfabritech facility at the University of Florida, and its director, Professor P. H. Holloway.

[1] S. Nakamura, T. Mukai, and M. Senoh, Appl. Phys. Lett. **64**, 1687 (1994).
[2] H. Amano, T. Tanaka, Y. Kunii, S. T. Kim, and I. Akasaki, Appl. Phys. Lett. **64**, 1377 (1994).
[3] M. Asif Khan, S. Krishnankutty, R. A. Skogman, J. N. Kuznia, D. T. Olson, and T. George, Appl. Phys. Lett. **65**, 520 (1994).
[4] T. P. Chow and R. Tyagi, IEEE Trans. Electron Devices **41**, 1481 (1994).
[5] T. Maksuoka, T. Sasaki, and A. Katsui, Optoelectron. Devices Technol. **5**, 53 (1990).
[6] N. Yoshimoto, T. Matsuoka, T. Sasaki, and A. Katsui, Appl. Phys. Lett. **59**, 2251 (1991).
[7] T. Nagamoto, T. Kuboyama, H. Minamino, and O. Omoto, Jpn. J. Appl. Phys. **28**, L1334 (1989).
[8] I. Akasaki, H. Amano, M. Kito, and K. Hiramatsu, J. Lumin. **68/49**, 666 (1991).
[9] S. Nakamura, M. Senoh, and T. Mukai, Jpn. J. Appl. Phys. **30**, L1708 (1991).
[10] C. R. Abernathy, P. Wisk, F. Ren, and S. J. Pearton, J. Vac. Sci. Technol. B **11**, 179 (1993).
[11] See, for example, S. Strite and H. Morkoc, J. Vac. Sci. Technol. B **10**, 1237 (1992).
[12] T. L. Tansley and C. P. Foley, Electron. Lett. **20**, 1066 (1984).
[13] S. J. Pearton, C. R. Abernathy, P. Wisk, W. S. Hobson, and F. Ren, Appl. Phys. Lett. **63**, 1143 (1993).

Downloaded¬25¬Mar¬2011¬to¬128.227.207.19.¬Redistribution¬subject¬to¬AIP¬license¬or¬copyright;¬see¬http://apl.aip.org/about/rights_and_permissions